ALICE 98-07
Internal Note/MAG
11 February 1998

Preliminary Design Report
for the
Dipole Magnet
of the
Muon Spectrometer

A L I C E Collaboration
Dipole Magnet Project Working Group

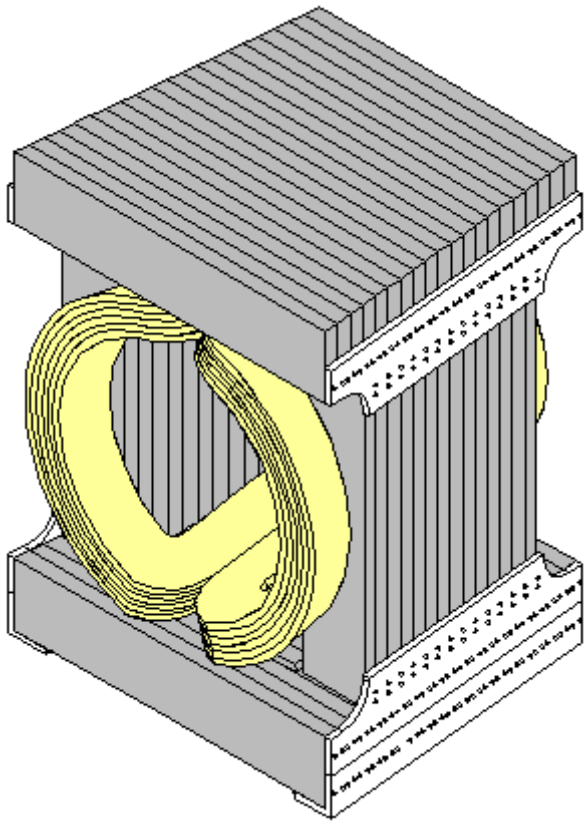

Content

1 Introduction

The ALICE Collaboration is preparing a dedicated heavy ion experiment based on ion-ion collisions as provided by the Large Hadron Collider LHC to be completed in the middle of 2005. An important part of the ALICE muon spectrometer is the dipole magnet providing the bending power to measure the momenta of muons. The ALICE Collaboration on its meeting in March 1997 evaluated different proposals for the muon magnet and chose a warm dipole magnet. The Dipole Magnet Project was formed in the March of 1997. The dipole magnet will be realised as a joint CERN-JINR project.

The ALICE dipole magnet is shown in Fig. 1-1. The overall dimensions of the magnet are 5 meters long, 6.2 meters wide and 7.7 meters high. The weight of the magnet will be ≈700 t.

The aim of this document is to fulfil the LHCC milestone to provide by the end 1997 the Preliminary Design Report for the Dipole Magnet. The document contains the preliminary technical description of the coil and yoke, the construction and the planned prototyping and modelling work.

The magnet parameters are given in Table 1-1.

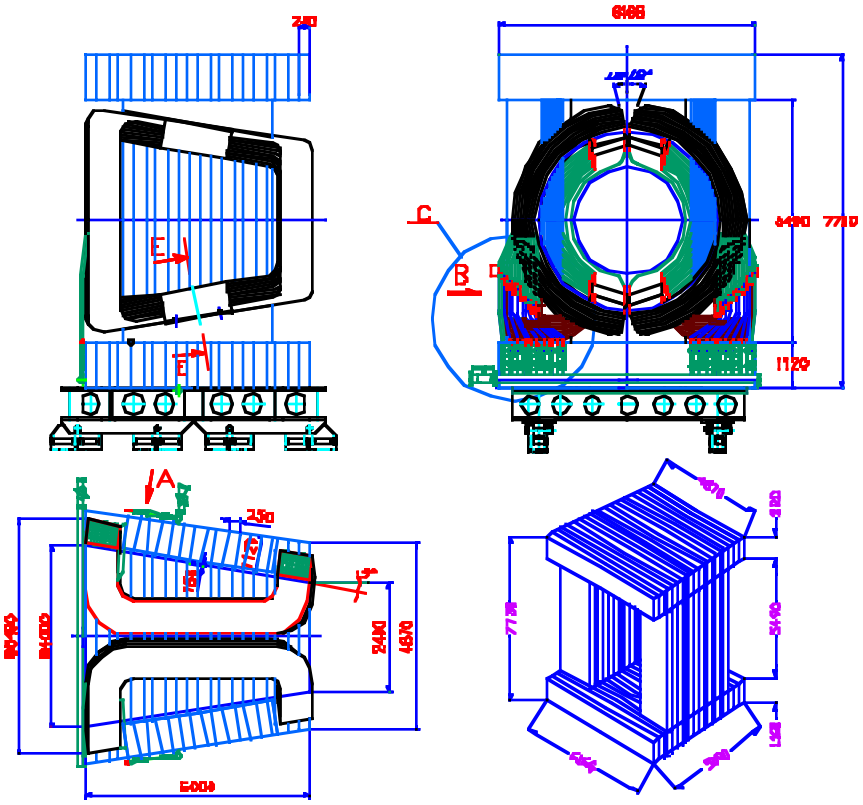

Figure 1-1. General view of the dipole magnet.

Table 1-1. Main parameters of the dipole magnet.

Item	Unit	Value
1. **Magnetic pole:**		
1.1 Max. field(x=y=0)	T	0.71(z=-0.6)
1.2 Field integral(z=±2.63,θ=0°-9°)	T×m	3.022-3.455
1.3 Integral ratio (max./min.)		1.14
1.4 Field integral(z=±2.63, θ=0°)	T×m	3.211
2. **Electric consumption:**		
2.1 Total Amp × turns	MA	1.938
2.2 Operating current	kA	6.06
2.3 Overall current density	A/mm^2	2.2
2.4 Consumed energy	MW	3.8
2.5 Source voltage	V	632
3. **Windings:**		
3.1 Features		Saddle conical
3.2 Aperture	m	∅ 2.7-4.3
3.3 Total length of magnet	m	5.0
3.4 Cross-section of winding	m^2	0.832×0.53=0.441
3.5 ***Al*** conductor mass	t	≈30
3.6 Perimeter windings	m	38.2
3.7 Volume windings	m^3	16.8
3.8 Total length of conductor	km	6.1
3.9 Layers/coil		10
3.10 Turns/layer		16
3.11 Turns/winding		320
3.12 Volumetric ratio ***Al***/winding		≈0.66
3.13 Conductor length/layer	m	305±25
4. **Conductor:**		
4.1 Material ***Al*** - *(99.5%)*		
4.2 Conductor cross section	mm^2	50 × 50
4.3 Channel, ∅	mm	29
4.4 Radius of the edge	mm	5.0
4.5 Cross-section area	mm^2	1818
5. **Insulation:**		
5.1 Insulation of conductor : adhesive Kapton tape, glass-fibre tape with epoxy resin	mkm mkm	40 × 4 250 × 4
5.2 Insulation of layer	mkm	250 × 4
6. **Cooling:**		
6.1 Cooling water supply	***l/s***	30.5
6.2 Pressure loss	Bar	5.2
6.3 Water heating: min, average, max.	^0C	26,30,34
7. **Magnet yoke:**		
7.1 Length	m	5.0
7.2 Volume	m^3	102
7.3 Yoke mass	t	700
7.4 Thickness of plates	m	0.25

2 Design parameters

The size and bending power of the dipole magnet are determined by the requirements on the mass resolution and geometrical acceptance. The mass resolution required for $\mu^+\mu^-$ pairs is of the order of $\sigma_m \leq 100$ MeV to distinguish the Υ family. The angular acceptance of the magnet is $2° < \theta < 9°$ which corresponds to a pseudorapidity range of $2.5 < \eta < 4$. An additional space of 15 cm radially is foreseen to house the support frames of the muon chambers (10 cm) and the coil bandage structure (5cm). The central field is 0.7 T and the field integral is 3.0 Tøm.
The magnet will be placed directly outside of the L3 magnet. The length of the magnet is 5 m. It will be mounted on a movable platform in order to be rolled back to gain access to the L3 doors and to allow mounting and demounting of the muon front absorber. Preliminary design studies for this platform are also under way.

The magnet will also be used as support for the muon absorber which will be supported by the front of the yoke.
The magnet will be powered by a DC power supply (the OPAL power supply is presently under consideration). The coil will be water cooled from a de-mineralised water plant at Point 2. The inlet temperature is in the range of 15-25°C. The inlet pressure at the magnet input water collector will be 8.2 bar. The water pressure at the water output collector of the magnet will be less than 2 bar.

3 Coil

3.1 Conductor

The coil will be made from a hollow aluminium conductor (Table 1-1 and Fig.3-1 and 3-2), extruded from aluminium of 99.5% purity. Impurities are Fe≤0.3%, Si≤0.3%, Cu≤0.015%. The total amount of impurities according to the standard must be ≤0.5%. Some characteristics from the Verkhnyaya Salda Metallurgical Production Association (VSMPO Joint Stock Co., Russia) are presented in Table 3-1. The conductor can be extruded as a single cut for the length needed to wind one layer of the coil. The welding of pieces of the conductor can consequently be avoided.

Table 3-1. Properties of aluminium

Item	Unit	Value
Max. electrical resistance at 20°C	Ohm×m	2.9×10^{-8}
Temperature coefficient of resistance at 20°C	$Grad^{-1}$	3.7×10^{-3}
Coefficient of thermal expansion at 20°C	$Grad^{-1}$	23.5×10^{-6}
Young's module	GPa	71
Tensile strength of annealed sample, $\sigma_{â}$	MPa	80
Yield stress of annealed sample, $\sigma_{0.2}$	MPa	30
Elongation, δ_{10}	%	40

Thermal processing of the aluminium consists in annealing with a temperature of 370÷400°C and cooling at ambient temperature. In the case, where it is required to take off strains only, the aluminium is annealed at 150°C.

The deformation of the cross section at a bend of the conductor essentially does not increase the hydraulic resistance of the channel. According to previous experience proved by the construction of coils for cyclotron magnets using similar conductor the radius of the bend could be as small as three times width of the conductor. The trapezoidal shape of the cross-section, arising from the bend of a small radius is eliminated by preceding machining at a prospective place of the conductor.

3.2. Structure of the coil

The coil consists of two half-coils of conical saddle shape (Fig.3-1). The coil follows as close as possible to the required aperture. This increases the filed homogeneity whilst the power dissipation is reduced. The cross section of the winding has rectangular shape (Fig.3-2). The longitudinal parts of the coil are rectilinear with the "snake" kind of transition to the front and rear parts. The front and rear parts of the coil have a half-cylinder shape. The bend of the conductor on the front and rear ends of the coil always occurs in a plane and smoothly passes into the conic frontal parts. During the process of coil manufacturing a number of special tools and filling components will be used for each turn to make sure that the conductor smoothly follows the designed bending geometry.

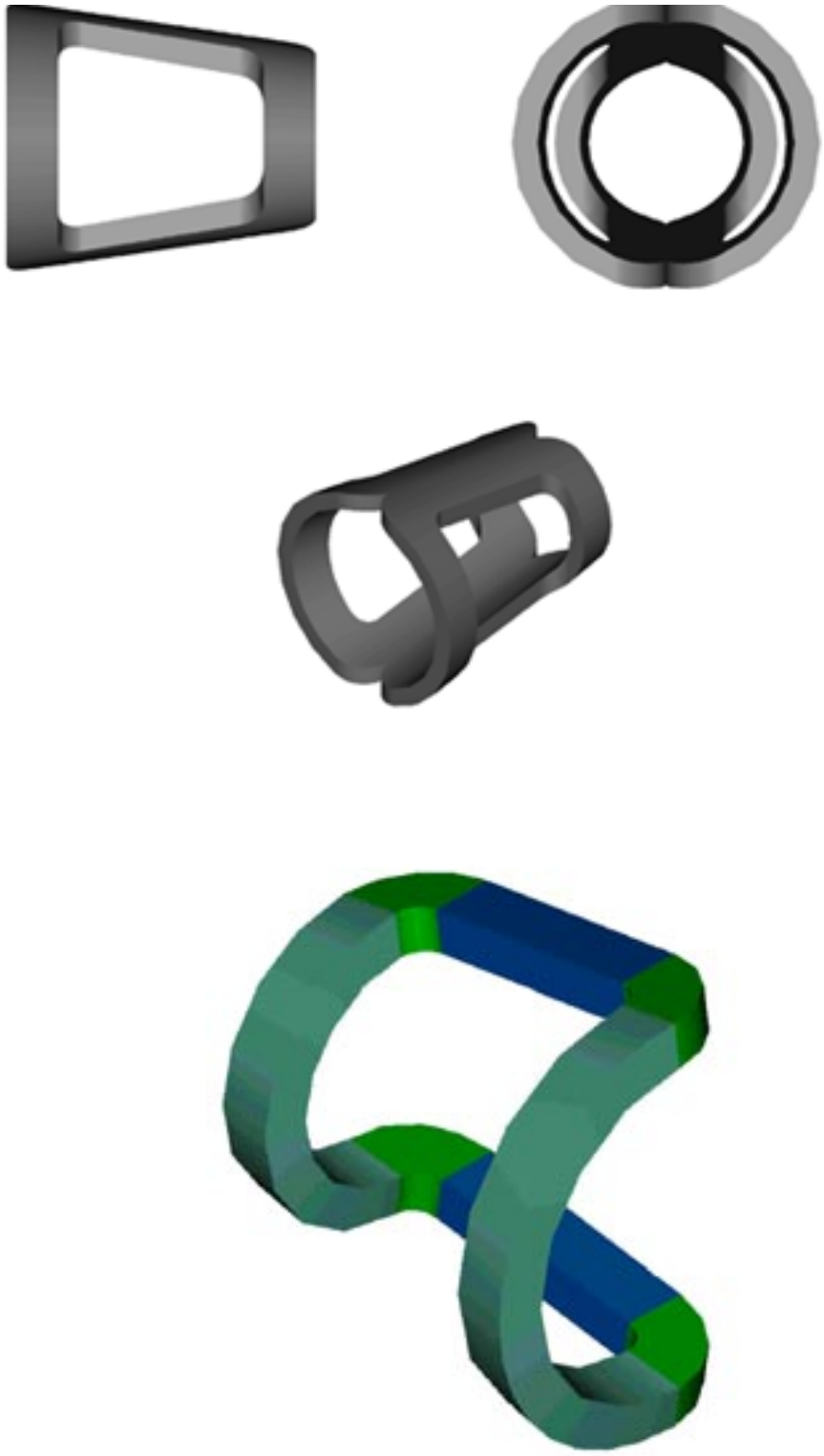

Figure 3-1. Coil consists of the two half-coils of conical saddle shape.

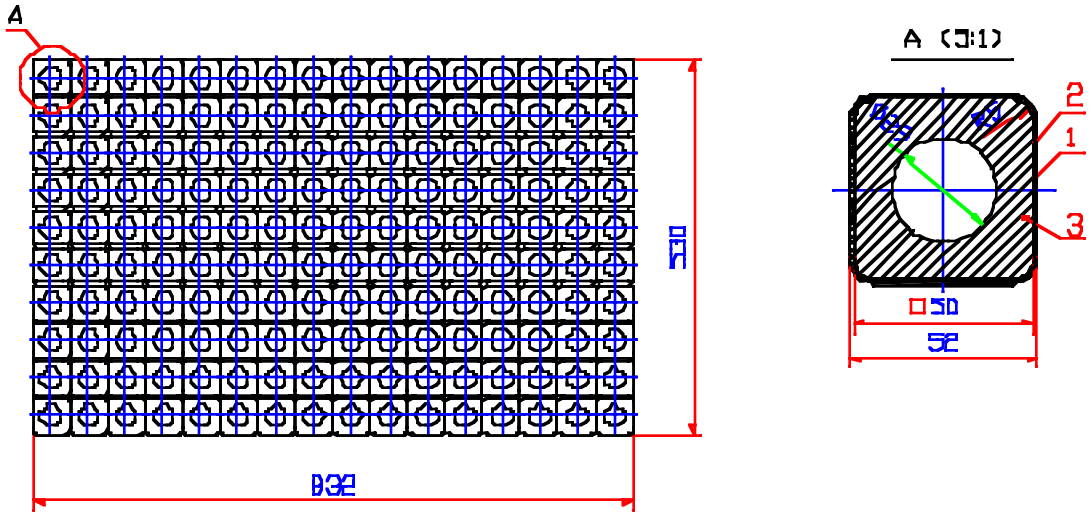

Figure 3-2. Cross-section of the conductor and the coil.

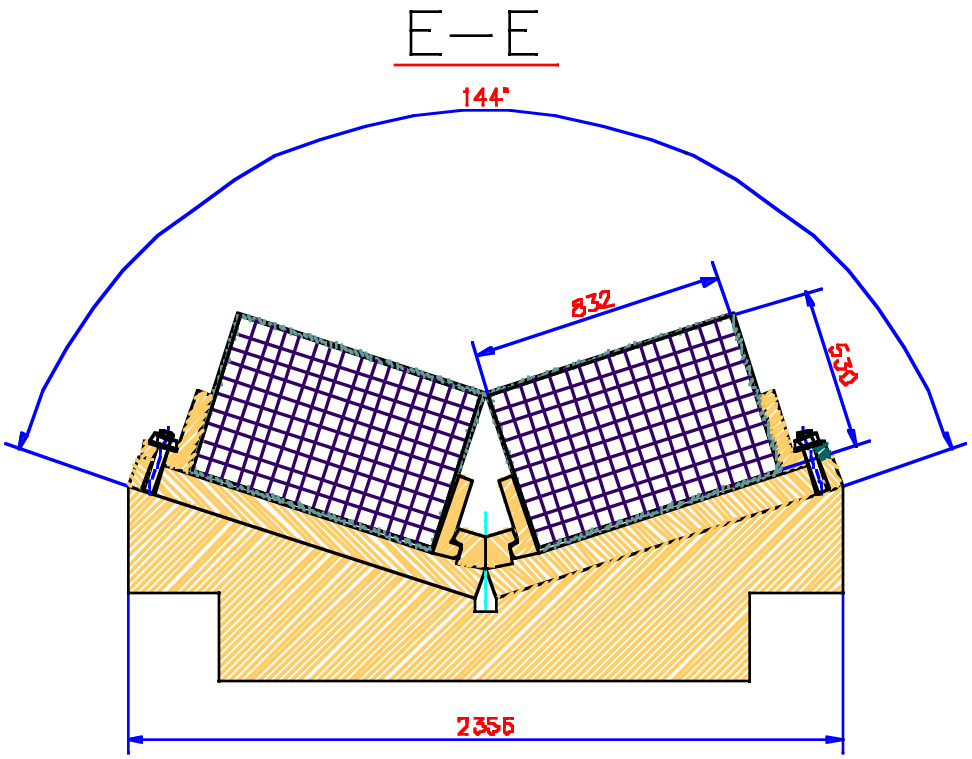

Figure 3-3. Fixation of the coil to the support inside the yoke.

The longitudinal parts of the half-coils will be mounted on supports in the yoke (Fig.3-3). They will be fixed to these supports in the median plane by bandages, where the largest electromagnetic forces occur at the coil.

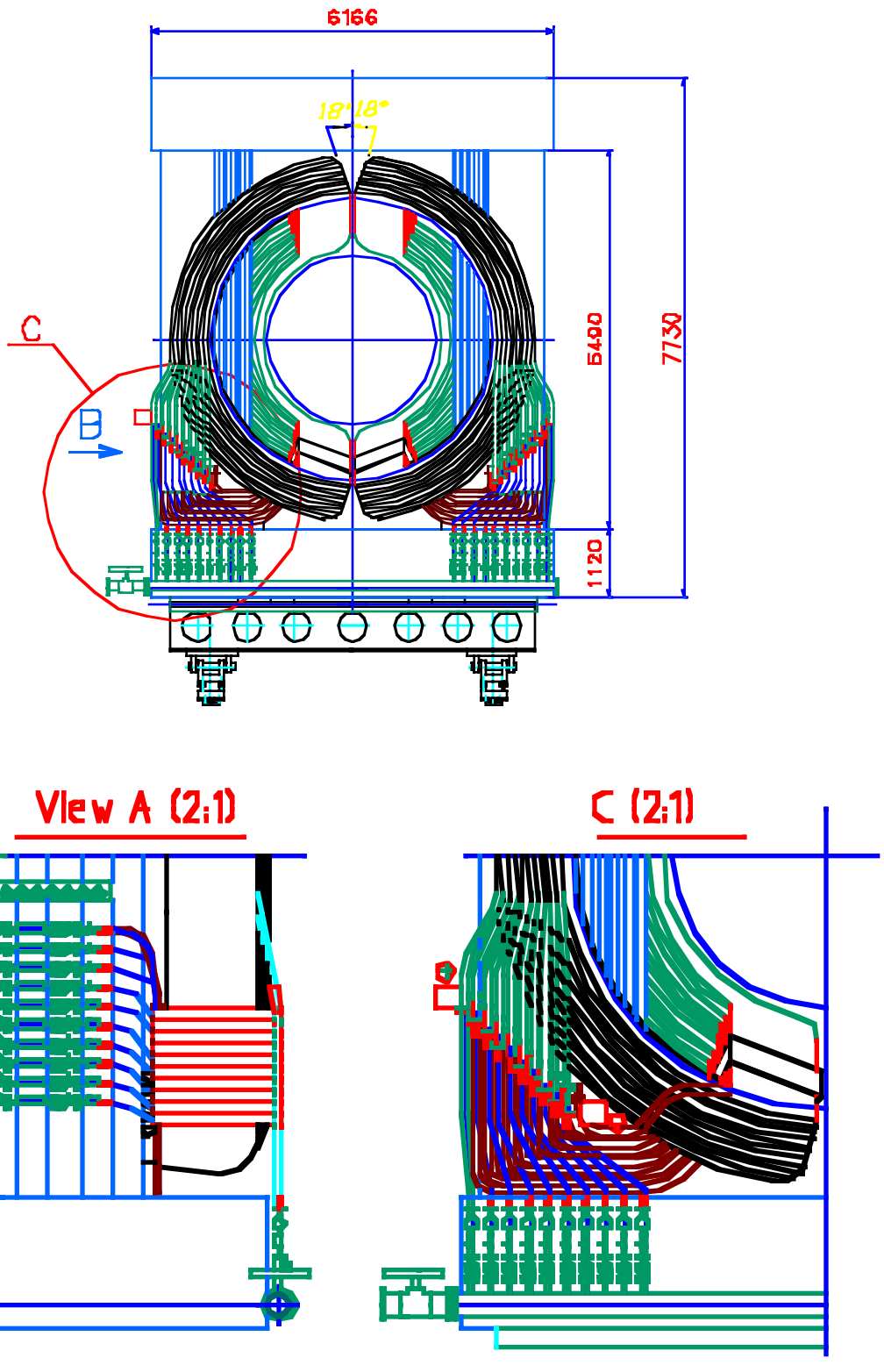

Figure 3-4. Electrical and water connections of the magnet. View C shows general view of electrical connections (in red) and part of the input water collector and water connectors (in green). View A shows from the side of the yoke one of water output collectors placed vertically (in green) and electrical connections between layers (in red).

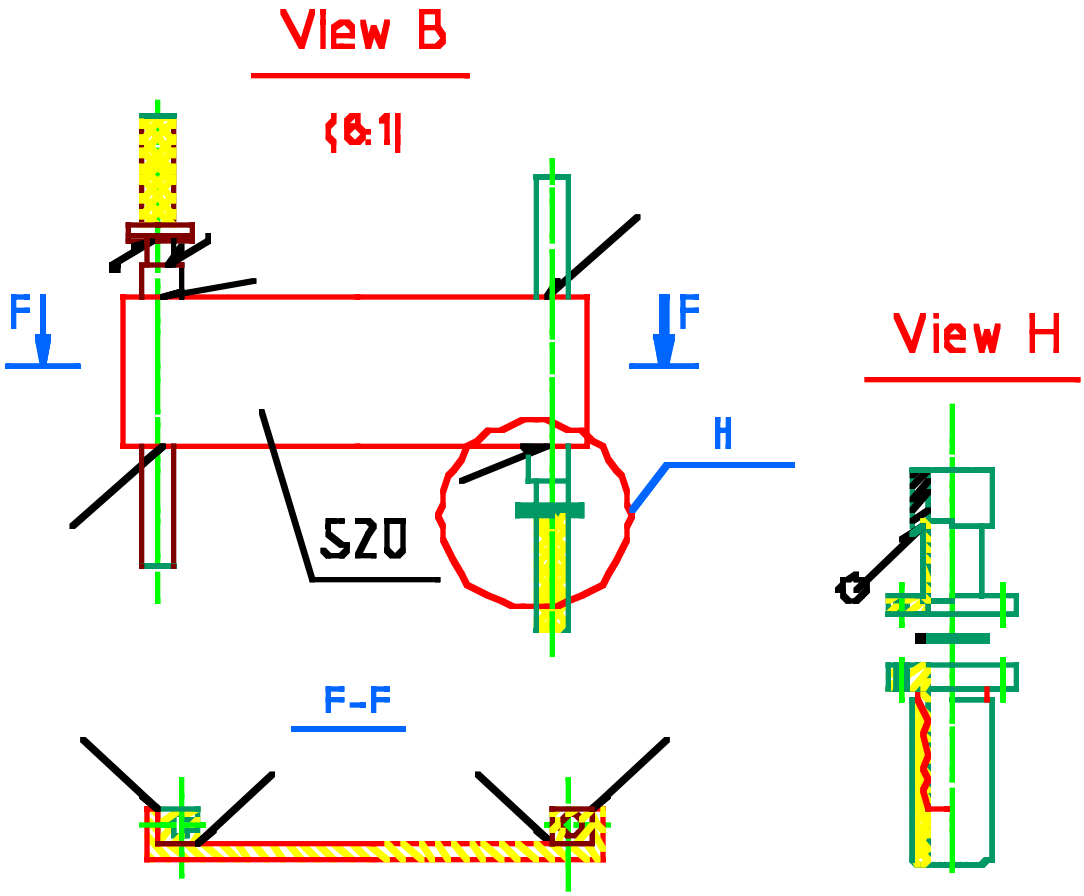

Figure 3-5. Details of electrical connections between layers of the half-coil (View B). Water connection is shown in View H.

The thermal expansion of the coil will be of the order of 2-3 millimetres during operation. The coil will, therefor, slightly move along the longitudinal supports. The fixation of the front parts of the coil to side walls of the yoke will be done with the help of ribs and an intermediate rubber sheets. The rubber will damp the coil movement.
Leads of the conductor (Fig.3-4 and 3-5) from each layer will be situated on the rear bottom parts of each half-coil. The electrical connections between layers are executed by welding *Al* pieces which are bolted to a current distributor.
Water inlets (shown in green on Fig.3-4 and 3-5) will be connected to the water collectors via flanges and rubber pipes. The input water collector is placed underneath at the rear end of the magnet. Output water collectors are placed vertically on both sides of the magnet and connected to each other below the coil.

3.3. Tooling and technology for the coil manufacture.

The coil will be made in the JINR workshop (Fig.3-6). The principle diagram of the winding procedure is shown in Fig.3-7. The rotating conical profile *2* with the electrical motor and reducer *3* is placed on the rotating milling machine table *1* (the diameter of 6.3 m is expandable to 14 m). Four removable spindles are placed on the profile to provide the bending angle during the coil winding. The bobbin with the conductor *5*, rollers *6* for the straightening and stretching of the conductor, devices *7* and *8* for the cleaning of the conductor and *9* for the wrapping of the insulation are situated on a base *4*. The conical hollow support is made from steel rings connected

placed on this support, fixed and machined to the required conical shape. During winding especially designed jigs of adequate radii and spacers will be used to shape the coil. A number of clamps and filling components especially designed for each turn of the winding will be used for fastening the conductor to the winding device.

Figure 3-6. The largest milling machine of the JINR workshop. The diameter of the rotating table is expandable up to 14 m.

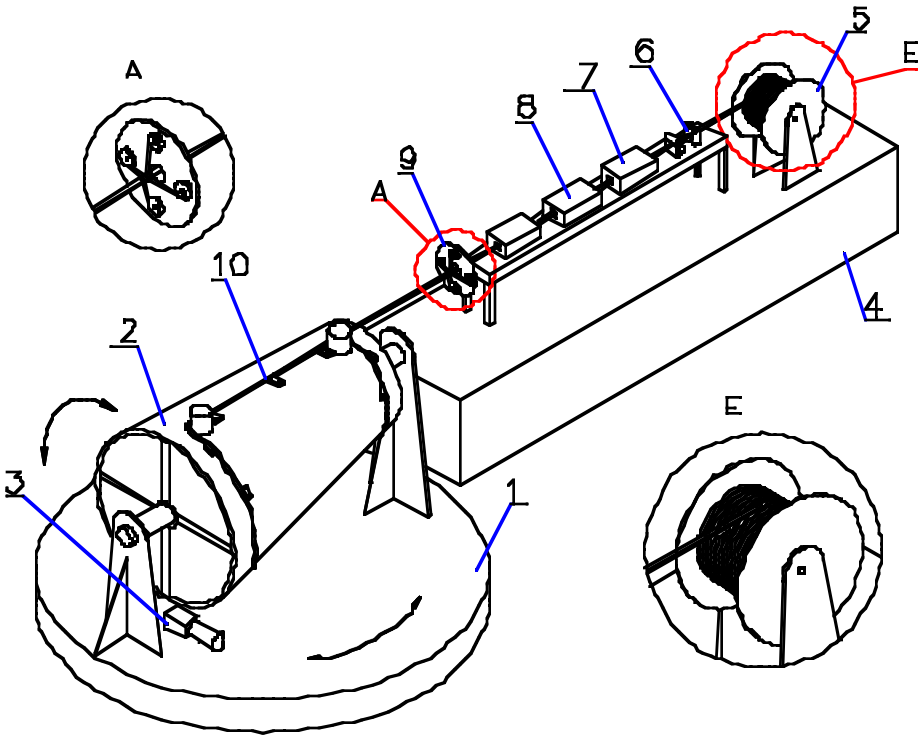

Figure 3-7. Principal diagram of the winding process and tooling.

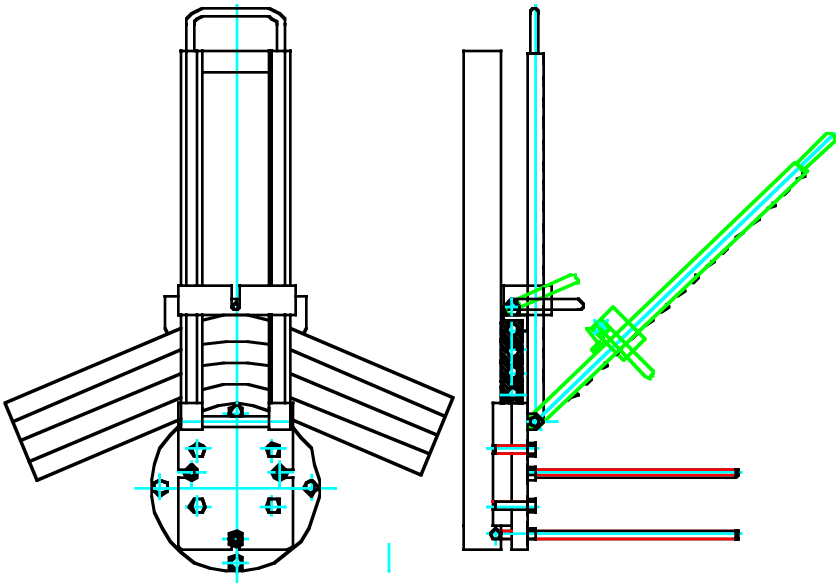

Figure 3-8. Example of the jig to use for the shaping of the winding in the corners. Four jigs fixed to four spindles in the corners of the winding.

The coil bandage and the support plate will serve also as support frame to remove the coil from the winding device and for further transportation purposes. To prevent the sticking of the epoxy resin to the surface of tools, intermediate sheets of the maylar - aclar or fluoroelastomer material will be inserted. The winding of the conductor will be performed by variable inclination and rotation of the milling machine table and the winding frame. The additional force on locations where the bend of the conductor occurs will be applied with the help of special jacks having

the required radii of curvature. The milling machine table is able to provide a force of the order of 40 tons.

3.4 Electrical insulation of the coil

Since we intend to use a power supply with low voltage (max.700V) theoretically only one layer of fibre-glass insulation with epoxy resin will be sufficient for the electrical insulation of the conductor. Mechanical strength of the insulation is an important problem because high stresses inside the coil may appear. The coil may be deformed due to tensions generated by differences in temperature along the winding of up to 30^0C. The value of such tension will depend on the difference in temperature, on the thermal expansion coefficient of the aluminium and the winding radius. For the insulation process the following considerations are taken into account:
- irregularity of the surface of the conductor in the range of 0.4-0.5 mm;
- real cross section of the conductor is not rectangular, since the edge is rounded with a radius of 5 mm.

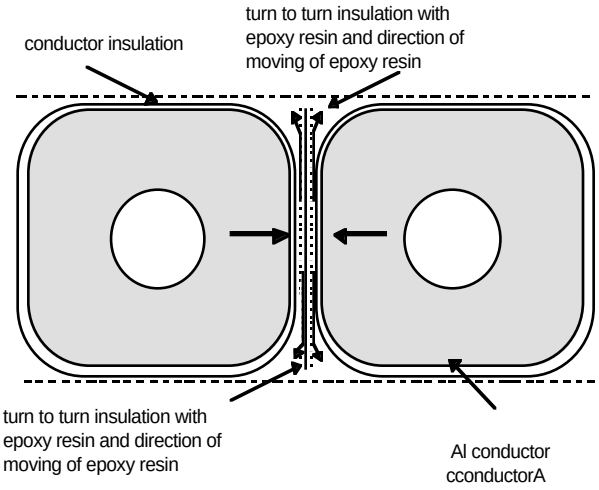

Figure 3-9. Insulation of the conductor.

A number of different insulation materials and epoxy resin were investigated (Table 3-2 and 3-3) in order to measure the adhesive force of the insulation to aluminium, possibilities to connect different types of insulation and possibilities to use the insulation in a continuous process of winding. In order to fill the spaces between layers of the coil, an inter-winding insulation of 0.1 mm thickness will be used with epoxy resin on each side of the insulation tape. During the winding process the epoxy resin fills the empty spaces (Fig.3-9 and 3-10).
To protect the flow off of the epoxy resin an additional filler could be used (SiO_2 with diameter of 20-30 μm about 15% weight). The following phases will be performed during the insulation of the coil:

1. Preliminary cleaning (brush cleaning). Even up and accurate cleaning (vibration grinder, abrasive paper).
2. Sandblasting .
3. Covering by the primary layer of epoxy resin.
4. Wrapping the wire insulation.
5. Place turn to turn insulation.
6. Place body insulation around the coil.
7. The resistance of the coil will be measured permanently during winding. The resistance between layers will be tested for 5000 V.

Table 3-2. Parameters of insulation from different producers

Producer	Tensile strength N/10mm	Adhesive forces N/10mm	Limit of temperature ^{0}C	Breakdown voltage V	Note
CMC N 84150, ASTAT, Germany	200	3	180	2500	adhesive
CMC N 84160, ASTAT, Germany	140-170	3	155	1500	adhesive
LESP-T, EIM, Latvia	130-230	-	-	-	thermo-shrink
LTSP-M, EIM, Latvia	200	3	155	3000	
Ergoterm 3, IZO-ERG,Poland	-	3	155	10000	
Ergoterm 2, IZO-ERG,Poland	-	9	155	7500	
Szkloflex, IZO-ERG,Poland		3	180	3000	
Ergopreg EF163 IZO-ERG,Poland	210	3	180	4500	

Table 3-3. Insulation materials based on Kapton film PML-1. Composition: Backing - Kapton film; Adhesive - synthetic rubber compound.

Item	Unit	Value
Thickness	mm	0.04; 0.06; 0.07
Dielectric strength	kV/mm	129
Volume resistance	Ohm×cm	1×10^{11}
Breaking strength	N/cm^2	45 56
Adhesion to backing (in initial state)	N/cm	0.3
Adhesion to Al (after thermal treatment)	N/cm	1.05
Curing conditions		5÷10 min at 80÷120 ^{o}C
Operating temperature range	K	123÷423

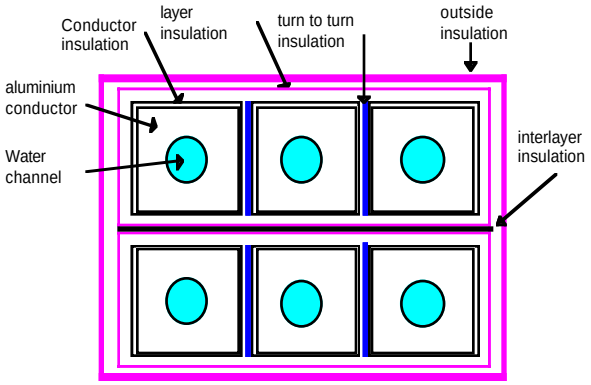

Figure 3-10. An example of the complete insulation of the coil.

After these steps the curing of the epoxy resin will be carried out (120 min / 160 ^{O}C). However, high dielectric strength requirement (~5kV) can not always be achieved by pure fibre glass tape reinforcement. Micro-cracks, which may grow under alternating load could create dielectric weak points. A mixed insulation of fibre glass tape and elastic plastic film, such as Kapton, is believed to solve this problem. The low-viscosity epoxy guarantees easy penetration and an excellent bond between the plastic film and the fibre-glass tape.

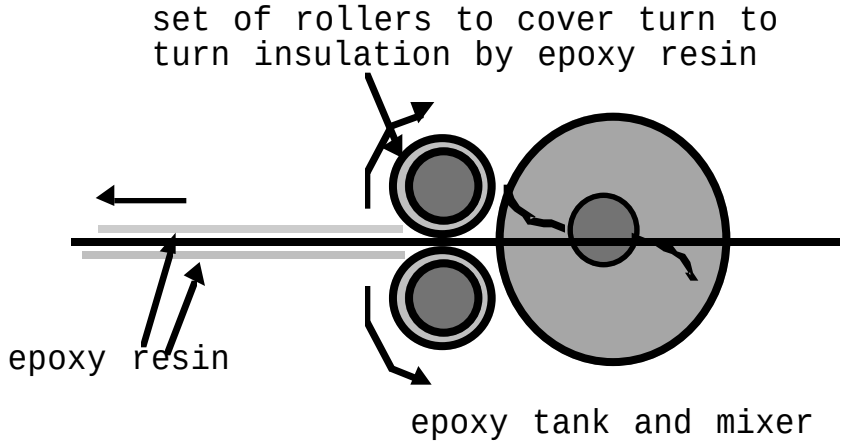

Figure 3-11. Schematic diagram of the device to moisturise the insulation tape with epoxy resin.

3.5 Radiation resistance of the insulation

The excitation windings will have to operate in the presence of ionising radiation. The admitted radiating dose on the winding of the magnet should be not less than 500 Mrad for 10 years - as for the regular magnet structure of the LHC accelerator. The proposed insulation, corresponds to a type of insulation tested at CERN (H.Schonbacher e. a., CERN 96-05, 1996). Samples of Orlitherm OH67 resin reinforced with glass-fabric respectively glass-fabric and Kapton tape were irradiated and subsequently the flexural strength and the modulus of the elasticity were determined as a function of the irradiation dose. The results of the tests which have been carried out at CERN show no significant influence of the irradiation up to a dose of 5×10^{9} rad.

4 The return yoke

The design of the yoke should satisfy the following criteria: robust, minimum of machining, easy assembly-disassembly and adapted to the 40 ton crane capacity in the ALICE experimental area. Most of the construction work will be done at the JINR (Dubna) workshop.

The yoke (Table 1-1 and Fig.1-1) will be constructed from low carbon steel slabs with a cross-section of 250∗1120 mm^2 produced at the Novolipetsk steel plant at Lipetsk city, Russia. The standard 240 and 250 mm, slab-thicknesses are produced in standard widths of 1120, 1290, 1370, 1440, 1550, 1640, 1660, 1710, 1850 mm and lengths of 5200 to 10500 mm. Some properties of the low carbon steel are given in Table 4-1. The upper and lower parts of the yoke are horizontal and the side walls follow to the conical shape of the coil.

Table 4-1. Properties of the low carbon steel.

Item	Unit	Value
Type of steel		08
Content of carbon	%	0.05÷0.12
Impurities	%	0.945÷1.445
Coefficient of thermal expansion in interval of (-183 ^{0}C) ÷(+20 ^{0}C)	$Grad^{-1}$	9.68×10^{-6}
Young's module at 20 ^{0}C	MPa	1.98×10^5
Tensile strength, σ_B	MPa	330
Yield stress, $\sigma_{0.2}$	MPa	200
Elongation, δ_5	%	33

Slabs will be rough machined in the factory. The precise machining will be done at the JINR workshop. Only joints between slabs will be machined. The slabs will be welded into modules not exceeding the weight limit of 40 tons.

To ensure the precise connection between slabs in view of the pre-assembly at JINR and the disassembly and assembly at CERN, the following manufacture procedure will be applied. The iron yoke "wall" modules will be bonded to each other by studs and nuts. Studs will be passing through saddle clips welded to adjacent modules. The lower and upper part of the yoke will be connected to the side walls by studs and nuts.

As an alternative the yoke could also be constructed from 100 mm thick plates. These plates are connected to each other into pancakes by the welding through drilled holes. Plates could be flattened if necessary by a press. The precision of the dimensions of such pancakes could be as good as 0.25 mm per meter of length. Good experience of the production of such pancakes exists at JINR workshop.

The final choice will depend on further optimisation of the iron yoke design.

5 Field calculations and forces

Extensive 3D field calculations were performed to study the magnetic field of the dipole magnet and its influence on the L3 magnet (W.Flegel and D.Swoboda, ALICE note 96-24, October 1996; V.I.Klyukhin e. a., ALICE note 96-44, March 1997). Field calculations were performed with the 3D finite element program TOSCA and with the 3D program IAMAG3D developed at JINR, Dubna and based on volume integral equations (P.G.Akishin e. a., ALICE note 96-06, April 1996; P.G.Akishin e. a., ALICE note 96-28, September 1996).
It was already shown in the Addendum to the ALICE Technical Proposal "The forward muon spectrometer of ALICE" (CERN/LHCC/96-32) that the dipole magnet field has a minor effect on the L3 field and therefore on the tracking performance in the TPC. These computations were done for a superconducting option of the magnet with the saddle shaped coil as well as for resistive coil designs.

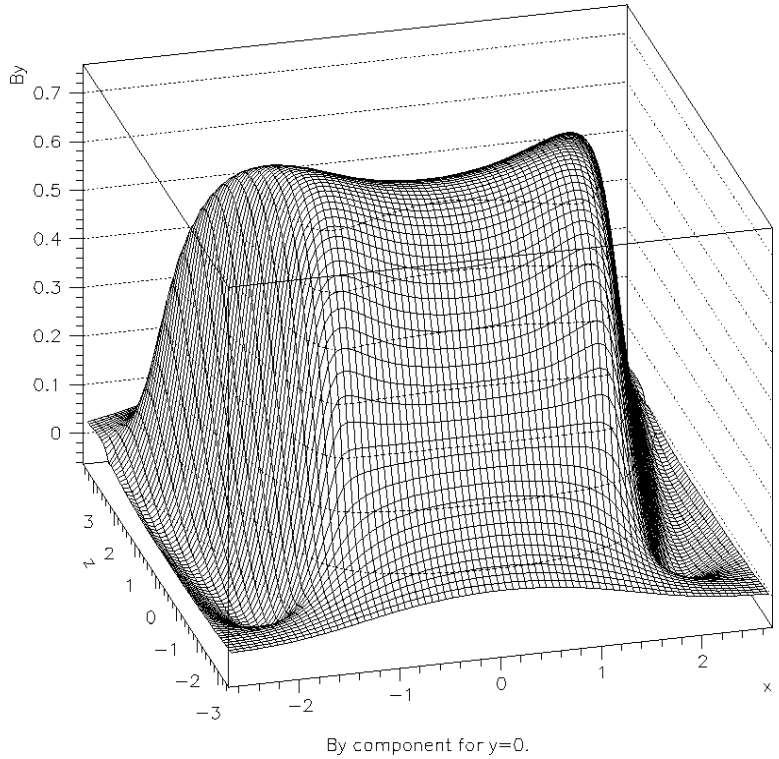

Figure 5-1. B_Y - component of the magnetic field at y=0.

Additional studies of the field of the warm magnet were performed with the IAMAG3D program. In Fig. 5-1 one can see the B_Y - component of the field for y=0 (in these computations the Y-axis is situated along the field direction and the Z-axis is situated along the beam direction). In Fig.5-2 the B_Y component of the magnetic field along the Z-axis is shown.
The magnetic field inside the iron yoke was studied for the particular design of the iron yoke. The slice representing the field in the iron 10 cm away from the median plane is shown as an example in Fig. 5-4. From Fig.5-4 it can be seen that there is no saturation of the magnetic field in the iron yoke. Further optimisation of the thickness of the yoke will certainly allow to reduce the amount of iron required.

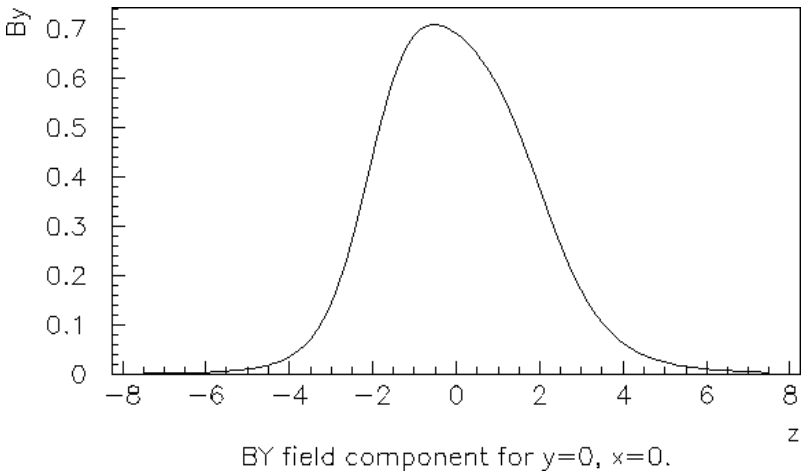

Figure 5-2. B_Y - component of the field along the Z-axis of the magnet.

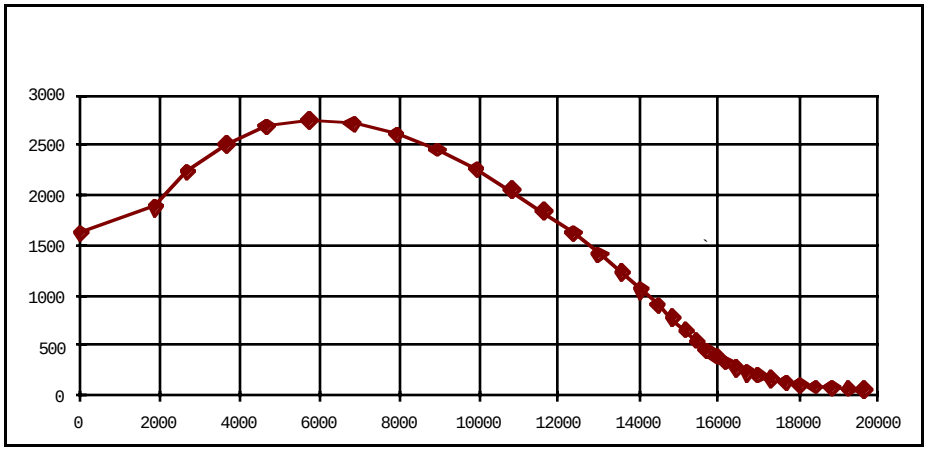

Figure 5-3. μB curve used in the 3D field calculations with the IAMAG3D code.

3D calculations of the magnetic field has made it possible to estimate the values of electromagnetic forces on the coil. In Fig.5-5 one can see the distribution of forces on the coil. Forces were calculated along the longitudinal parts of the coil with ***Z***=æ1.6 m from the magnet centre and within the angular range of 0 0.8 rad. The resulting values of the forces presented were computed as sums of the corresponding values related to finite parts of the coil (F=∑f).
They are as follows:
F_X 99 ton; F_Y 50 ton; F_{Z1} 17.6 ton; F_{Z2} 18.2 ton; F_{Z3} 17 ton;
$f_{r1} = 54.5 \cdot 10^4$ N / rad; $f_{r2} = 63.8 \cdot 10^4$ N / rad.

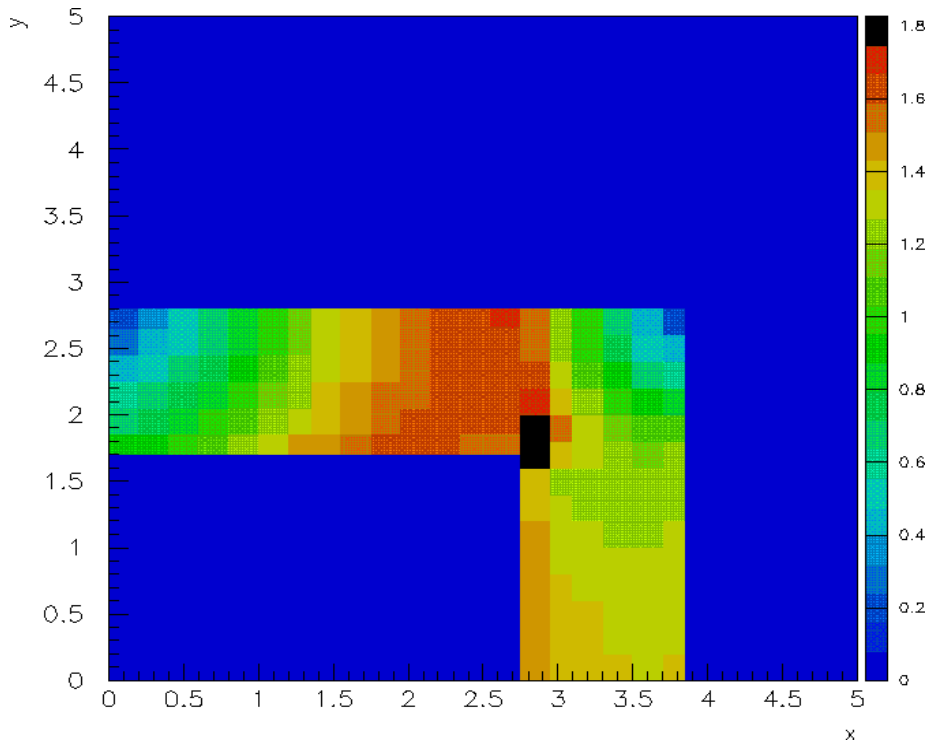

Figure 5-4. Field saturation in the iron yoke. The Y-axis situated along the dipole field direction. X and Y are in meters. The magnetic field scale is shown on the right side of the picture. The largest value of the magnetic field in the iron is about 1.8 T.

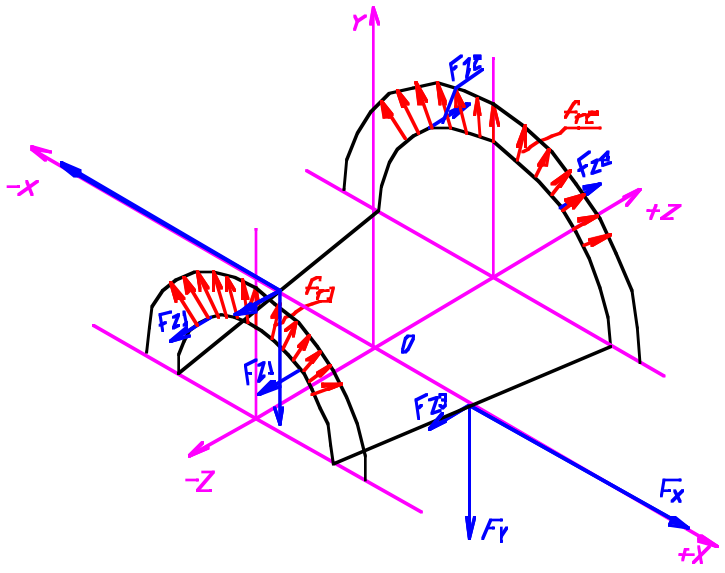

Figure 5-5. Schematic view of the electromagnetic forces acting on the coil (Y-axis is situated along the field direction).

6 R&D and prototypes

6.1 Conductor material tests

It is expected that after extrusion the heat treatment of the conductor as well as quality checks of the internal aperture with the help of a steel ball will be performed at the factory. During the manufacturing of the coil at JINR the conductor will be reeled out from the bobbin and pass through a number of rollers which will result in an increase of its hardness.

The following questions have to be addressed and checked on the basis of the *Al*-conductor of 52x52 mm cross-section presently available at JINR and a real conductor of 50x50 mm which has to be obtained from the factory:

- rigidity of the conductor after mechanical hardness and heat treatment;
- force needed for the twisting of the conductor by 9 degrees;
- force needed for the bending of the conductor to the minimal radius of 250 mm;
- change of dimensions of the conductor cross-section after the bending;
- checking of the internal aperture of the conductor after bending and twisting with the help of a steel ball.
- roller calibrator of the size of the conductor.
- heat treatment.
- mechanical cleaning of the conductor(sandblasting).
- welded and bolted electrical contacts.
- water pipe joints.

6.2 Electrical insulation of conductor

In the proposed coil the insulation material has a double purpose: electrical insulation and mechanical rigidity of the winding. The good quality of the insulation on the whole length of about 5000 m of the conductor can only be ensured with the help of special wrapping machines and strict quality control. The chosen technology and materials should ensure the absence of damage during bending, twisting and friction of the conductor in the manufacturing process. All these aspects should be investigated on a real conductor with several types of insulation material and appropriate epoxy compounds. The following tests are foreseen:

- dielectric tests.
- insulation resistance.
- mechanical strength.
- action on various components and processes (varnishing of conductor; felt; curing temperature; epoxy resin etc.).

6.3 Prototypes

To verify the construction of the 3D coil it is essential to check the key questions and aspects of the coil manufacturing. The present status of the R&D work is given below. In 1998-99 we plan in addition to gain more experience in working with the full size conductor. It is planned to make a prototype winding to check the following:

- Make the full cross-section of the straight part of the coil including the insulation and impregnation.

- Make the test winding of a few turns and layers of the conductor around a corner on the smaller radius of the cone support frame. For this purpose one quarter of the cone frame at the smaller radius should be constructed.

It is also foreseen to build a working model of a half-coil (see APPENDIX 3).

6.4 **Present status of R&D**

6.4.1 Bending of the conductor.

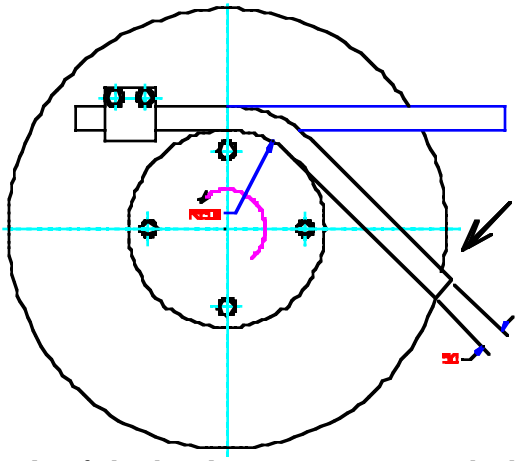

Figure 6-1. The principle of the bending experiment with the 52x52 mm conductor carried out at JINR.

Figure 6-2. The device used for the bending of the conductor.

A simple test was made to bend the 52x52 mm conductor. The principle of this bending experiment is shown in Fig.6-1. The device used is shown in Fig.6-2. The piece of hollow *Al* conductor was taped with ordinary insulation and covered by epoxy resin. One end of the sample and a roller were fixed on the rotating table. The table was rotated very slowly. The sample was bent around the roller. After that a second piece of conductor was fixed to simulate the next turn of the winding over the "wet" surface of the first one. The second sample was bent in the same manner as the first one. A pusher (see Fig.6-2) was used to push the second sample towards

the first one because some small slit remained after the bending was performed by hand. As one can see, the insulation was not destroyed after this simple test. In Fig.6-3 the pusher is shown with the thin spacer of G10.

6.4.2 Study of the deformation of the conductor with the rapped insulation.

During manufacturing of the coil a special “pusher-tool” will be used in the corners, where the conductor will be bend with the smallest radii. It is important to know how the insulation will behave under locally applied pressure and what value of the local deformation of the aluminium conductor could take place. To study these questions the aluminium conductor of 52x52 mm with taped insulation and epoxy resin was prepared. A special press device (Fig.6-5) was used for these tests. The force was applied to the conductor (Fig.6-4) via the hard steel roller (95 mm) with a pressure of up to 10 tones. The following diagram (Fig.6-3) shows the dependence of the conductor deformation pressure for different types of insulation and as a function of spacers.

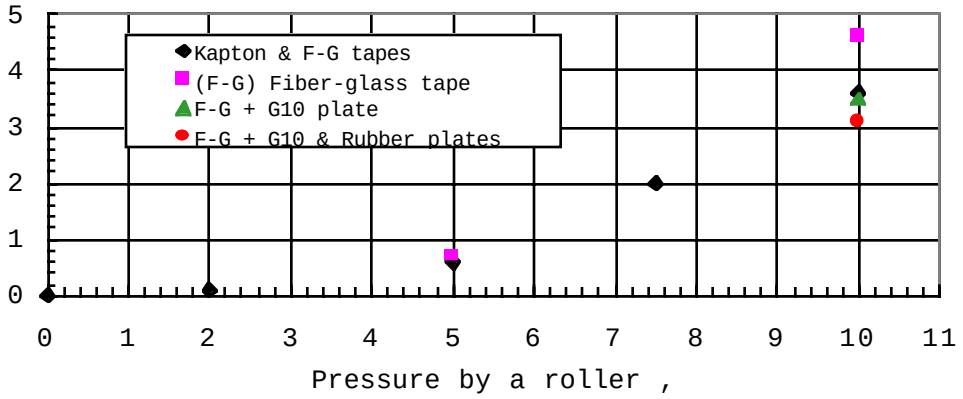

Figure 6-3. Conductor deformation with different types of the insulation (Kapton tape: 4x0.04 mm, Fibre-glass tape: 4x0.25 mm) and additional spacer materials (G10 plate: 2x0.5 mm, Rubber plate: 2mm).

On the basis of the measurement of the electrical resistance and external inspection it was concluded that the insulation had not been damaged even under 10 ton pressure. The electrical resistance of the insulation was measured (>100 MŒ, 30V) during the pressing procedure by contact between the Al conductor and the steel roller. The deformations were measured geometrically with the roller on the flat surface and on the deformed surface. The analysis of the test results has shown that the introduction of flexible spacers like G10 and rubber plates allow substantially reduce the deformation of the surface of the aluminium conductor. For a pressure of up to 2 tones no deformation of the surface of the conductor was detected. Thus it is possible to bend the aluminium conductor with the taped insulation at the required force and with the help of the additional pressing tool through flexible linings. The active part of the pressing tool could consist of independent rollers with a force of 1-2 tones on each roller.

Figure 6-4. The sample of the conductor after the deformation test. Small caves seen on the surface of the conductor that was taped by Kapton film and standard insulation. Insulation was not destroyed up to a pressure of 10 ton.

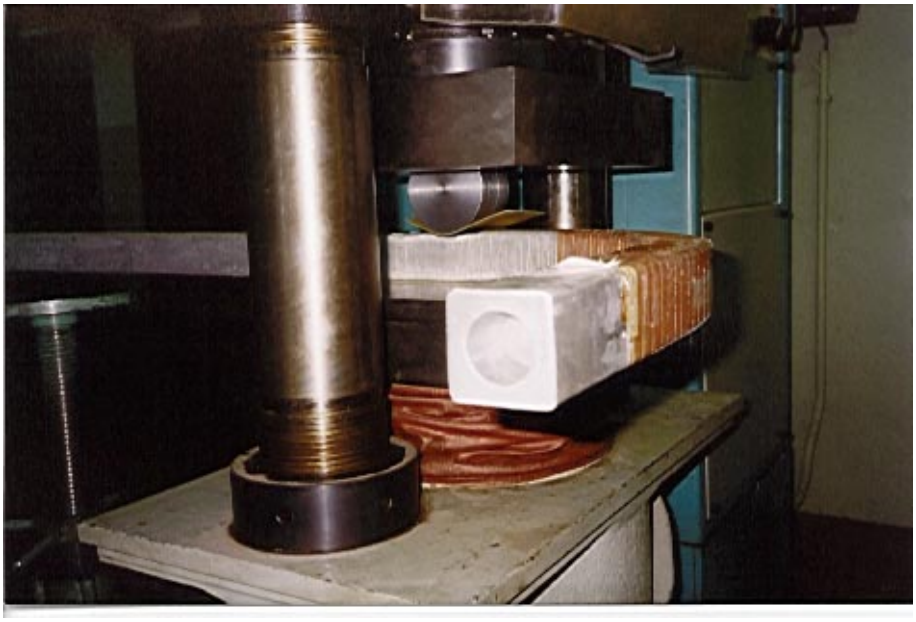

Figure 6-5. The press device that was used for the deformation test, showing the roller, spacer and Al conductor. The thickness of the insulation is 1 mm (white) and 1.16 mm (brown).

APPENDIX 1

Power consumption of the coil

The power consumption can be estimated as

$$\boldsymbol{P = j^2_{Al} \times \rho(t) \times V_{Al}},$$

If $\boldsymbol{V_{Al} = k \times V_{win.}}$ and $\boldsymbol{j_{Al} = j_{win.} \times k^{-1}}$,

then $\boldsymbol{P = j^2_{win.} \times V_{win.} \times \rho(t) \times k^{-1}}$.

Where

$j_{win.}$ [$A \times m^{-2}$] - current density in the coil;
j_{Al} [$A \times m^{-2}$] - current density in the conductor;
$\rho(t)$ [Ohm×m] - specific resistance of the conductor, as function of temperature;
V_{Al} [m^3] - volume of the conductor in the winding;
$V_{win.}$ [M^3] - volume of the winding;
k - filling factor of the winding;
P [Wt] - dissipated power;

$\rho(t) = \rho(20^{\circ}C) \times [1 + \alpha(20^{\circ}C) \times (t - 20^{\circ}C)]$,

where $\alpha(20^{\circ}C)$ $Grad^{-1}$ - temperature coefficient for resistance at 20 $^{\circ}C$. For aluminium $\alpha(20^{\circ}C) = 3.7 \times 10^{-3}$ $Grad^{-1}$ and $\rho(20^{\circ}C) = 2.9 \times 10^{-8}$ Ohm×m (Table 3-1).

From 3D - field calculations (Table 1-1) the following values are known: $j_{win.}=2.2 \times 10^6$ $A \times m^{-2}$, $V_{win.}=16.8$ m^3. We take k=0.66. Maximal temperature of cooling water at input of the coil, t_1 = 25 $^{\circ}C$, and the maximal allowable heating is $\Delta t=30°C$. Thus the maximal temperature of the water on the outlet collector of the coil is 55$^{\circ}C$, and average temperature on the winding is about 40$^{\circ}C$. With these assumptions we obtain:

$$\rho(40^{\circ}C)=2.9 \times 10^{-8} \times [1+3.7 \times 10^{-3} \times (40-20)]=3.11 \times 10^{-8} \text{ Ohm} \times \text{m}.$$

Thus:

$$P = 2.2^2 \times 10^{12} \times 16.8 \times 3.11 \times 10^{-8} \times 0.66^{-1} = 3.83 \times 10^6 \text{ Wt}.$$

APPENDIX 2

Cooling water requirements of the coil

1 Cooling of the coil

Consumption of cooling water:

$$\boldsymbol{U = P \times C^{-1} \times \Delta t^{-1}},$$

where C = 4.18 $W \times s \times g^{-1} \times Grad^{-1}$ - thermal capacity of water.

$U = (3.83 \times 10^{6}) / (4.18 \times 30) = 30.5 \times 10^{3}\ g \times s^{-1} = 30.5\ l/s.$

With a diameter of the cooling hole of the conductor of d=29 mm, the velocity of water in the channel is

$w = (4 \times U) / (2 \times \pi \times d^{2} \times n) = (4 \times 30.5 \times 10^{-3}) / (2 \times \pi \times 29^{2} \times 10^{-6} \times 10) = 2.32\ m \times s^{-1},$

where n=10 - number of layers in the half-coil.

For isothermal flow in a straight round pipe the loss of pressure due to friction is

$$\boldsymbol{\Delta p = (\lambda \times \gamma \times w^{2} \times L)/(2 \times d)},$$

where Δp[Pa]; γ[kg/m^{3}] - density of a liquid, w [m/s] - average velocity; L[m] - length of pipe; d[m] - internal diameter of ~~a~~ pipe; λ- friction coefficient.

The Reynolds number is given by

$$\boldsymbol{Re = w \times d \times \gamma \times \eta^{-1} = w \times d \times \nu^{-1}},$$

where
$\eta = 66.6 \times 10^{-6}[kg \times s \times m^{-2}] = 6.53 \times 10^{-4}[kg \times s^{-1} \times m^{-1}]$ -dynamic viscosity of water at 40°C;
$\nu = \eta \times \gamma^{-1}$ - kinematics viscosity [m^{2}/s];
$\nu = 6.53 \times 10^{-7}\ m^{2} \times s^{-1}$.
$Re = (2.32 \times 29 \times 10^{-3}) / (6.53 \times 10^{-7}) = 1.03 \times 10^{5} >> 10^{4}$,
i.e. turbulent flow.

To calculate λ with the Reynolds number in the range of $1 \times 10^{5} \div 1 \times 10^{8}$ for pipes having smooth walls of a round cross-section the following expression is used

$$\lambda = 0.0032 + 0.221 / Re^{0.237}.$$

In our case: $\lambda = 0.0032 + 0.221 / 15.45 = 0.0175.$

For an average layer of the coil L=305 m and λ=0.018,

$\Delta p = (0.018 \times 10^{3} \times 2.32^{2} \times 305) / (2 \times 9.8 \times 0.029) = 5.2 \times 10^{4}[kg/m^{2}].$

So: $\Delta p = 5.2[kg/cm^{2}].$

The length of the conductor in the outer layer of the coil is 330 m. Hence the consumption of the cooling water will be higher. Calculations show that in the outer layer at $\Delta p = 5.2\ kg/cm^2$ the heating of the water will be about 34ŁC.

2 The choice of the optimum cooling hole diameter in the conductor

The input conditions for the optimisation are the water flow and speed, necessary to remove the heat generated by the current through the aluminium conductor. The given parameters are ampere-turns of winding or the current of 6060 A and $30^{O}C$ temperature difference on whole length of the conductor in one layer. In the following diagram the dependence of hydraulic resistance of the water channel on its diameter and length of the aluminium conductor is shown.

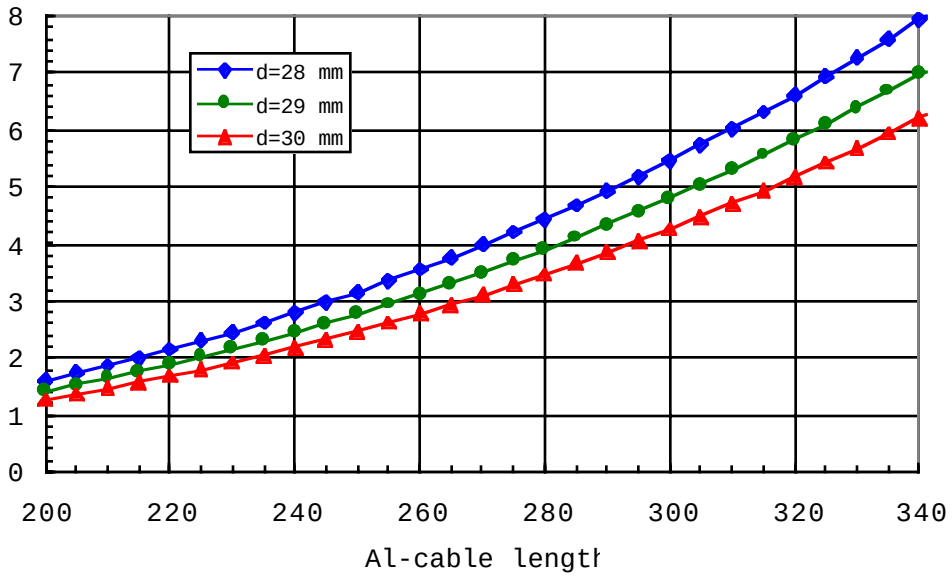

Figure A2-1. Hydraulic resistance of water channel in conductor of 50x50 mm at 6060A current.

APPENDIX 3

Coil model

1 Introduction

There is a great experience of constructing various magnet systems at the JINR workshop. However, most of recently built magnets have copper coils and were rather small in size in comparison to the ALICE muon magnet. Consequently, it will be inevitable to test the coil manufacturing process prior to the final design of the magnet. We consider of high importance to carry out the modelling of all components of this system. On the basis of an aluminium conductor of 18x18 mm with a hole of 8 mm in diameter we plan to make a model of the coil in 1:3 scale. The parameters of the proposed model are given in Table A3-1.

2 The objectives of the model

- winding of 6 layers with 10 turns each;
- realistic manufacturing procedure using a conical support frame with fixing tools and jigs;
- straightening the conductor by rollers;
- handling of the bobbin with the conductor;
- water and electrical connections;
- cleaning of the conductor and wrapping of the insulation;
- insulation quality checks.

Figure A3-1. The winding device that could be adapted to wind the coil model in 1:3 scale.

Table A3-1. Main parameters of the model of the coil in the scale M1:3

Item	Unit	Value
Electric consumption :		
Total Amp × turns	kA	50.2
Operating current	A	836
Overall current density	A/mm^2	2.2
Consumed energy	kW	6.8
Source voltage	V	7.0
Winding:		
Features		Saddle conical
Aperture	m	∅ 0.8-1.33
Total length of coil	m	1.67
Cross-section of winding	mm^2	.193×.118=.228
Al conductor mass	t	0.285
Perimeter windings	m	~6.4
Volume windings	m^3	0.146
Total length of conductor	m	384
Layers / coil		6
Turns / layer		10
Turns / winding		60
Volumetric ratio ***Al***/winding		~0.72
Conductor length / layer	m	54
Conductor:		
Material ***Al*** - *(99.5%)*		
Conductor cross section	mm^2	18 × 18
Channel ∅	mm	8.0
Radius of edge	mm	1.5
Cross-section area	mm^2	272
Insulation:		
Different types of insulation: Kapton tape, fibre-glass tape, polyester felt and epoxy resin		
Cooling:		
Cooling water supply	***l/s***	0.024
Pressure loss	Bar	0.47
Water heating	^0C	30

3 The basic goals

- modelling of the manufacturing technology ;
- investigation of the coil functioning with the current on;
- thermo - cycling of the coil up to 1000 times;
- checking the dimensions of the model winding after the manufacturing process;
- checking the insulation during the winding process by the generation -resonance method;
- vacuum impregnation of the coil;
- experience in the design and manufacturing of required tools;
- tests of the model in the stress situations;
- checks of the insulation and the conductor by cutting the coil.